*Journal of Microscopy, 2009*
*Received 29 May 2009; accepted 21 July 2009*
doi: 10.1111/j.1365-2818.2009.03317.x

# Full spectrum filterless fluorescence microscopy

M.J. BOOTH, A. JESACHER, R. JUŠKAITIS & T. WILSON
*Department of Engineering Science, University of Oxford Parks Road, Oxford OX1 3PJ, United Kingdom*

**Key words.** Coherence, fluorescence microscopy, polarization, spectrum, structured illumination.

**Summary**

In conventional microscopes, fluorescence emission is separated from the backscattered illumination using the Stokes shift, whereby the emission occurs at a longer wavelength to the excitation. Such separation is usually achieved through a combination of wavelength filters that divide the spectrum into mutually exclusive excitation and emission bands. It is therefore impossible in these microscopes to access the full excitation/emission spectrum of the specimen in a single image. We report on a microscope that acquired fluorescence images using illumination across the spectral range 450–680 nm; the full emission spectrum was detected simultaneously across the same range. The microscope was also combined with structured illumination optical sectioning to give three-dimensionally resolved images with improved background rejection. Full spectrum fluorescence images of biological specimens are demonstrated. As this system is more versatile than the standard fluorescence microscope, it could be of benefit in many fluorescence imaging applications.

## Introduction

Fluorescence microscopy is used widely in biological imaging and is particularly useful when combined with methods such as confocal, multiphoton or optical sectioning microscopes to image multiple fluorescent species in three dimensions (Pawley, 2006). As the fluorescence intensity is usually orders of magnitude smaller than the illumination intensity, the emission can only be detected if it is separated from the backscattered illumination light. This separation is usually achieved through a combination of excitation, dichroic and emission filters, but this permits only a limited region of the full excitation/emission spectrum of the specimen to contribute to a single image (Fig. 1). The coverage of the excitation spectrum is even more restrictive in laser-based microscopes, where it is confined to discrete laser lines.

Correspondence to: Martin J. Booth. Tel: +44 1865 283306; fax: +44 1865 273905; e-mail: martin.booth@eng.ox.ac.uk

Separation using the wavelength shift is therefore a fundamental limitation in these systems. To achieve full benefit from a broadband illumination source and to access the full excitation/emission spectrum, a different form of separation must be employed. Full spectrum fluorescence detection has been performed, for example, using time gating to differentiate between excitation and emission light (Ye *et al.*, 2007). This was not however compatible with an imaging system. Using the polarization and coherence properties of fluorescence emission, we have developed a microscope that can acquire fluorescence images using illumination across the spectral range 450–680 nm; the full emission spectrum can be detected simultaneously across the same range.

Polarization filtering was used to discriminate between fluorescence and back-reflected light. Fluorescence emission usually exhibits a large degree of polarization anisotropy, whereas reflected light retains the polarization state of the illumination (Lakowicz, 1999). By using linearly polarized illumination and a crossed analyzer, the contrast between the fluorescence and the scattered light is increased as the analyzer cuts out a significant proportion of reflected illumination. Specular reflections, for example from the microscope slide or lens surfaces, are linearly polarized and are mostly filtered out. Although scattering from small features exhibits a degree of depolarization (Born & Wolf, 1983), the majority of backscattered light is removed.

The difference in coherence properties of the illumination and the fluorescence provides a further possibility for separation. Uniform widefield illumination can be generated by illuminating a point in the pupil of the objective lens using a spatially coherent source. Illumination light reflected back from planar surfaces, such as the microscope slide, will follow a reciprocal path through the objective, again forming a point in the pupil. This point can be blocked by a small beam stop. On the other hand, fluorescence emission is mainly incoherent and isotropic so fills the objective pupil. Only a small proportion of this will encounter the beam stop. This spatial coherence filtering therefore increases the contrast between fluorescence and illumination light. This principle has been used to produce linear illumination in a high speed slit scanning

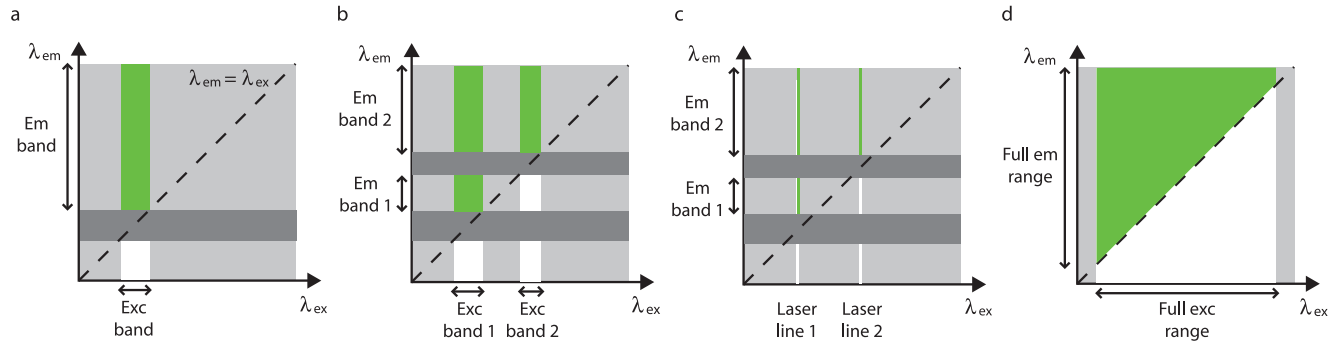


**Fig. 1.** The regions of fluorescence excitation/emission spectra accessible in different microscopes: (a) conventional microscope with one excitation band, limited by excitation and emission filters; (b) conventional microscope with two filter-limited excitation bands; (c) laser-based microscope using two excitation lines and (d) full-spectrum filterless microscope, limited only by the output wavelengths of the source. The accessible regions are marked in green, assuming that $\lambda_{em} > \lambda_{ex}$. The white vertical bands show the available excitation wavelengths, whereas the dark horizontal bands indicate the sections of the emission spectrum that are inaccessible due to filtering of the excitation wavelengths. Key: Em – emission, Exc – excitation.

microscope, albeit in conjunction with laser illumination and emission filtering (Wolleschensky *et al.*, 2006).

The full-spectrum microscope requires broadband, spatially coherent illumination, which was provided by a photonic crystal fibre-based white light supercontinuum (WLS) source. These sources have provided much greater freedom in laser scanning microscopy, removing the previous restriction to laser lines (Dunsby *et al.*, 2004; Betz *et al.*, 2005; McConnell *et al.*, 2006; Frank *et al.*, 2007; Owen *et al.*, 2007; Booth *et al.*, 2008). However, demonstrations of these sources in fluorescence microscopy have all employed some form of wavelength filtering, so were unable to access the complete excitation/emission spectra in a single exposure.

The microscope was also combined with structured illumination (SI) microscopy, enabling the acquisition of optically sectioned, three-dimensionally resolved images using a conventional microscope (Neil *et al.*, 1997, 2000; Gustafsson, 2000). In this technique, the image of a grid is projected onto the specimen producing a one-dimensional sinusoidal excitation pattern in the focal plane of the objective lens. The resulting image, consisting of both in-focus and out-of-focus fluorescence emission, is acquired by a camera. Several images are taken, each corresponding to a different grid position. As the grid pattern appears only in the focal plane, it is possible to extract an optical section from the spatially modulated component of the images via a simple calculation. The optical sectioning process has the effect of further reducing the contribution of out-of-focus scatter.

## Experimental methods

The microscope configuration is illustrated in Fig. 2(a). Broadband illumination (450–2000 nm) was provided by a Fianium SC450-2 WLS source. The output light was passed through a filter, removing all wavelengths longer than 680 nm. The resulting beam was expanded and passed through a Glan Taylor polarizer before being focused by a 50 mm focal length lens. The focussed beam was reflected off a small inclined mirror (diameter 3 mm) positioned close to the back aperture of the objective lens (Zeiss PlanNeoFluar, 40×, 1.3 NA, oil immersion). These components were placed to ensure that the illumination beam formed a focal spot in the pupil plane of the objective, thereby producing wide-field illumination of the specimen. Light emitted by the specimen was collected using the same objective lens. Some of the light passing through the pupil was obstructed by the mirror and beam stops, the remainder passed through to a polarizing beam splitter (PBS). The component of polarization at 90° to the input polarization was reflected by the PBS then imaged using a 400 mm tube lens on to the charge-coupled device (CCD) camera (Andor iXon EMCCD, 512 × 512 pixels, used in conventional detection mode). The other path from the PBS accommodated conventional K öhler illumination using a Exfo X-Cite light source. Operation equivalent to a non-polarizing microscope was achieved by placing a film polarizer rotated to 45° between the PBS and the objective lens. Spectral measurements of the specimen could be taken by replacing the CCD camera with an optical fibre, which was connected to an Ocean Optics USB2000 spectrometer.

SI was implemented by inserting a patterned mask into the object-conjugated plane between the first polarizer and the following lens. The grid pattern (pitch 80 μm) on the mask was imaged onto the specimen to produce the SI. The mask was translated using a piezo stage in order to obtain images with a shifted illumination pattern. The illumination distribution in the pupil plane of the lens, being the Fourier transform of the grid pattern, consisted of several points corresponding to the orders of a diffraction pattern. As the 0th, 1st and -1st diffraction orders are required to produce a sinusoidal illumination pattern, this places a lower limit on the size of

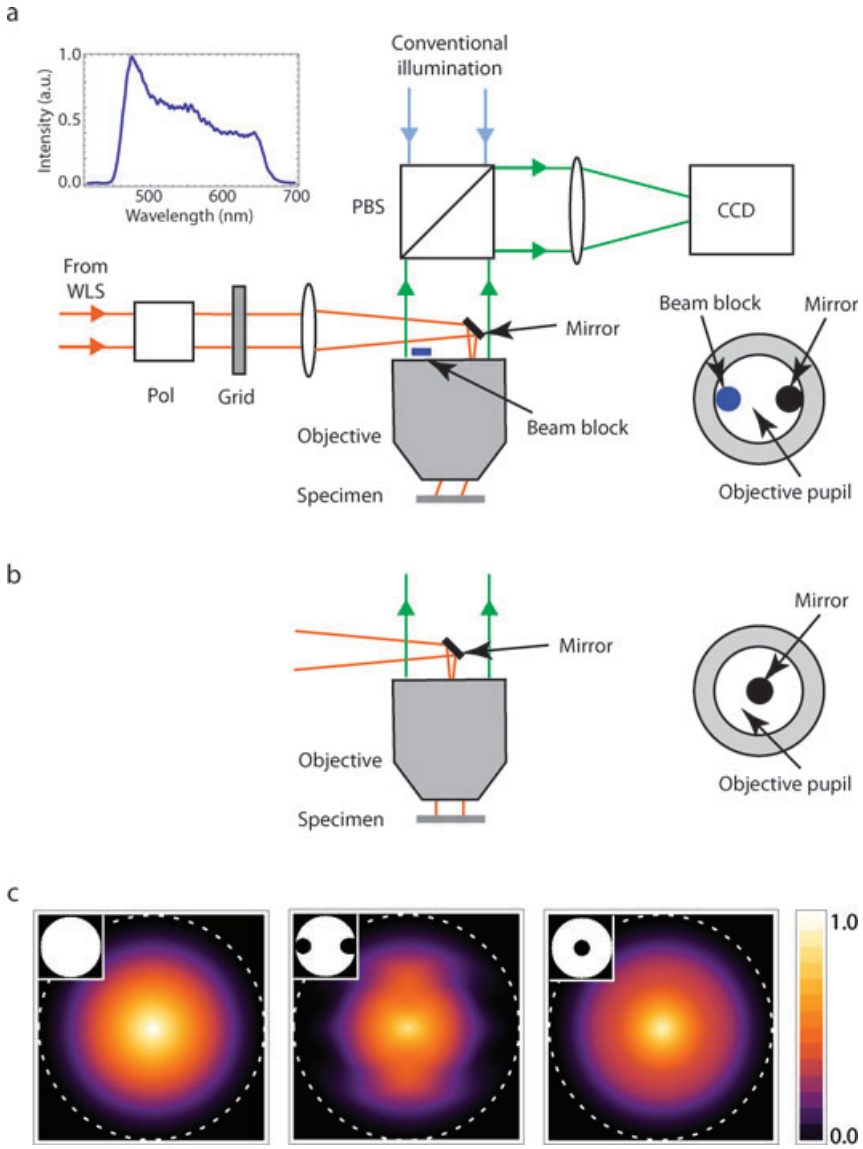


**Fig. 2.** (a) Schematic diagram of the microscope (Pol - input polarizer, PBS – polarizing beam splitter). The inset (top left-hand side) shows the spectrum of the WLS after filtering. The diagram (bottom right-hand side) shows the arrangement of the mirror and beam block in the back aperture of the objective lens. (b) Alternative positioning of the mirror. (c) Calculated OTFs for the free and obscured pupils. The pupils are shown in the insets. The dotted line indicates the region of support of the conventional OTF.

the mirror. In our case, the 3rd diffraction orders were also reflected, although this has no effect on the final sectioned images. The thickness of the optical section produced by this SI imaging system, defined as the full-width half-maximum of the axial response to a thin fluorescent sheet, was calculated to be 3.3 μm (Karadaglic & Wilson, 2008). SI images were extracted from three acquired frames using the algorithm of Cai *et al.* (2003).

Ideally the mirror and beam stops should be placed in the pupil plane of the objective lens. However, as the pupil plane of most objectives is located within the lens barrel, the mirror and stops must be placed as close as possible to the back aperture of the lens. Two possible positions for the mirror are shown in Figs 2(a) and (b). For the case shown in Fig. 2(b), the mirror was placed on the optic axis and acts dually as a beam stop. It was assumed that the mirror supports did not obscure the pupil. In the other case, the mirror was placed at the edge of the pupil and a beam stop (a 3 mm plastic disc) was placed diametrically opposite. This latter configuration (Fig. 2a), which was used to obtain the following results, was found to exhibit reduced back reflections from the lens components, due to the larger surface angles encountered along the light path. This principle of this effect is illustrated in Fig. 3, by comparing an illumination point on the optical axis with one at the periphery of the lens

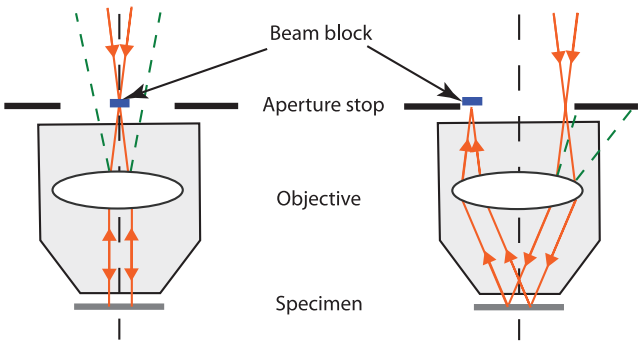


**Fig. 3.** Illustration of the effects of two illumination configurations showing the illumination and specimen reflections (red) and the spurious reflections from lens elements (green dashed). On the left, illumination is focussed to a point on the optic axis; on the right, the illumination is focussed at the edge of the objective pupil.

pupil. When illuminating at the periphery, the inclination of the lens surfaces (here simplified to a single element for illustrative purposes) cause the reflected light to be deflected at high angles, away from the pupil, so the light is blocked by the lens casing. On the other hand, when the illumination enters the lens on the optic axis, the reflected light passes back through the pupil and contributes to the detected intensity.

The spatial filtering in the pupil also has an effect on the imaging properties of the microscope. This can be quantified by calculation of the optical transfer function (OTF) as the auto-correlation of the pupil function (Born & Wolf 1983). The pupil functions and corresponding OTFs are shown in Fig. 2(c) for an unobstructed pupil and for the two illumination configurations discussed above. It can be seen that the spatial filtering changes the shape of the OTF, but causes only minimal change to the region of support. The imaging properties of the microscope are therefore not significantly altered.

## Results

The various contributions to the imaging process in this microscope are illustrated in Fig. 4 using images of a fluorescent pollen grain (Carolina w.m. 30- 4264 (B690)). Image (a) shows the pollen grain using conventional illumination in coherent reflection mode with a closed condenser aperture. Note the large background signal contributed by reflections from the microscope slide. Part (b) shows a conventional crossed-polarizer reflection image of the specimen. The image shows suppressed background reflection and consists predominantly of depolarized scattered light from the pollen grain.

For Fig. 4 images (c)–(f), the WLS was used to illuminate the specimen via the pupil plane mirror. In image (c), the input polarizer was removed and background light was filtered solely using the spatial filtering effect of the pupil plane beam blocks. The pupil plane filtering provided good rejection of the specular

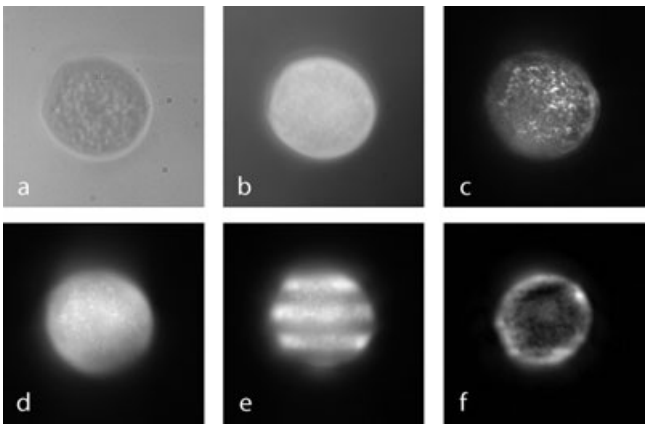


**Fig. 4.** Contributions to the imaging process. Each image shows the same focal plane in a single fluorescent pollen grain: (a) conventional illumination reflection image, (b) conventional image with crossed polarizers, (c) WLS illumination with pupil plane filtering, (d) WLS illumination with pupil and polarization filtering, (e) single image for structured illumination and (f) sectioned image from structured illumination.

reflections from the microscope slide. The bright regions in the centre of the pollen grain are due to scattering features. Image (d) was taken after insertion of the input polarizer. Note that neutral density filters were also changed and that this image shows 1000 times lower intensity than image (c). This difference is mostly due to the extinction of the reflected light so that the image consists mainly of fluorescence. Image (e) is a SI image taken after insertion of the grid in the illumination path. This is one of the three images required for the SI calculation. Part (f) shows the final SI sectioned image of a single plane through the pollen grain.

The major benefit of this microscope is the ability to simultaneously access the full excitation/emission spectrum. Full spectrum images are illustrated in Fig. 5, which shows non-sectioned and SI sectioned images obtained using the microscope from three fluorescent specimens: (a) an autofluorescent pollen grain, (b) a multiply labelled muntjac fibroblast cells (Molecular Probes FluoCells prepared slide #6), (c) multiply labelled mouse intestine specimen (Molecular Probes FluoCells prepared slide #4). The optical sectioning effect of this microscope is clearly visible in the images (a) and (c). In (b), where the specimen is relatively thin, it can be seen that the SI process reduces the out-of-focus background signal, which is predominantly due to residual reflected light.

The full spectrum microscope can be used in combination with any detector or spectrometer channels without restriction to those bands permitted by dichroic filters. We demonstrated this versatility by using emission filters (without excitation filtering) to verify the full spectrum nature of the images. This is illustrated in Fig. 6, which shows conventional (non-SI) images of bovine pulmonary artery endothelial cells (Molecular Probes FluoCells prepared slide #1). Two of the

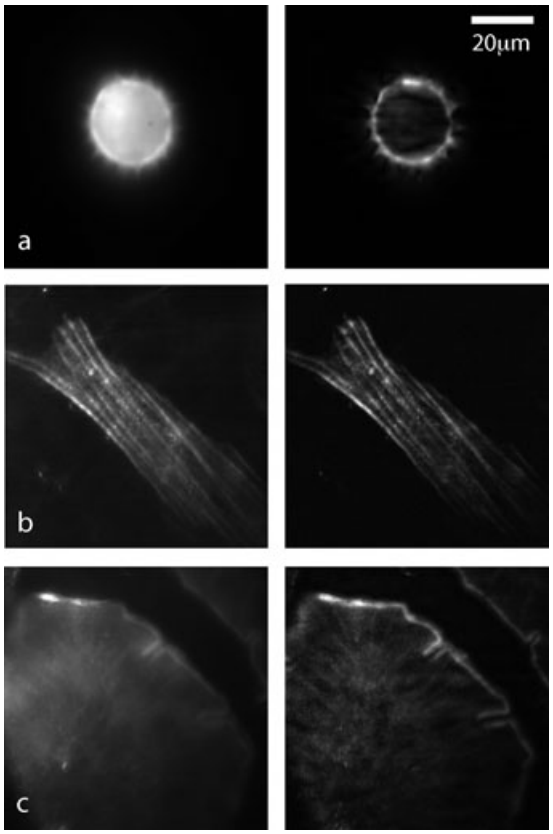


**Fig. 5.** Full-spectrum, conventional (left-hand side) and sectioned (right-hand side) images of fluorescent specimens: (a) pollen grain, (b) muntjac fibroblast cells and (c) mouse intestine section.

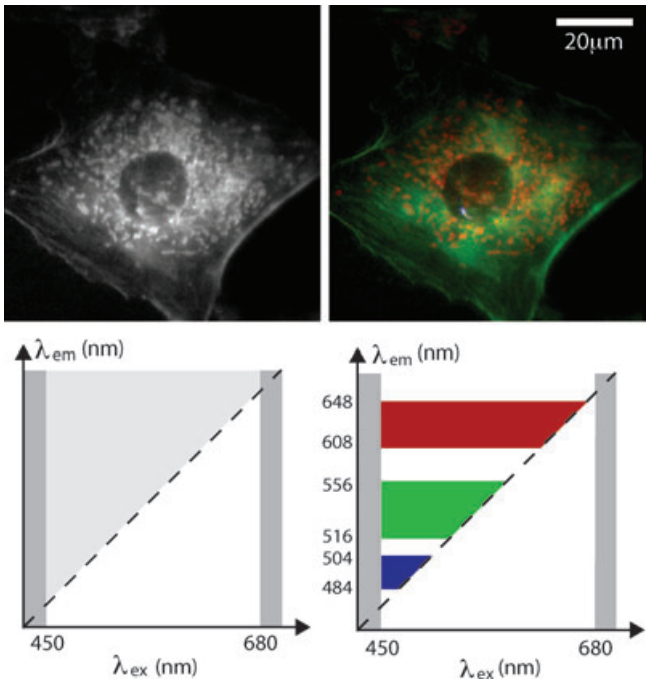


**Fig. 6.** Full-spectrum fluorescence image of bovine pulmonary artery endothelial cells (left-hand side) and compound image (right-hand side) constructed from three separate detection channels: red 608–648 nm, green 516-556 nm and blue 484–504 nm. The charts show schematically the regions of the excitation/emission spectrum used in the images.

three fluorescent dyes in this specimen could be excited using the available illumination wavelengths: BODIPY FL phallacidin (absorption peak 505 nm, emission peak 512 nm) and MitoTracker Red CMXRos (absorption peak 579 nm, emission peak 599 nm). The first image shows the intensity image of all emission from the specimen. In order to verify that this image was composed of the emission from both of the markers, band pass emission filters were placed sequentially in the detection path. The red and green channels were recorded using appropriate band pass filters. A further blue channel was recorded; as there should be no appreciable fluorescence in this range, any detected signal in this channel should only be due to scattering. The compound image of these three channels shows good correspondence with the full-spectrum image, clearly indicating that the two fluorophores were simultaneously imaged. Only a small number of features can be seen in the blue channel, indicating that the majority of the full-spectrum image is due to fluorescence with only a small contribution arising from scattering.

In some specimens there may be weak fluorescence from certain markers that is obscured by stronger nearby fluorescence or by residual scattered light. For such specimens, weak fluorescence channels could be extracted using a combination of excitation and emission filters, but still without the need for a dichroic beamsplitter. Fig. 7 shows (non-SI) images of three types of fluorescent spheres: blue (diameter 1 μm, excitation maximum 430 nm. emission maximum 465 nm); green (1 μm, 505 nm, 515 nm); red (2 μm, 580 nm, 605 nm). The green and red beads showed strong fluorescence, whereas the blue beads were very weakly excited, as there was little overlap between the absorption spectrum (maximum at 430 nm) and the illumination wavelengths produced by the WLS (>450 nm). An additional emission filter (484–504 nm) was included to retrieve the weak blue channel. Although this configuration is likely to have lower overall efficiency, if compared to an appropriately optimized excitation/emission/dichroic combination, this approach removes the requirement for multiple dichroics if multiple fluorescence channels are used.

For the images shown in Figs 6 and 7, the residual backscattered light formed a background signal that was uniform across the field of view. This uniformity indicates that the background was mainly due to reflections outside of the focal region, for example from the lens surfaces or the coverglass. The mean background level was measured by imaging a region of the specimen away from any objects. This level was then subtracted from the resulting images and the contrast was adjusted. The same procedure was followed separately for each channel when emission filters

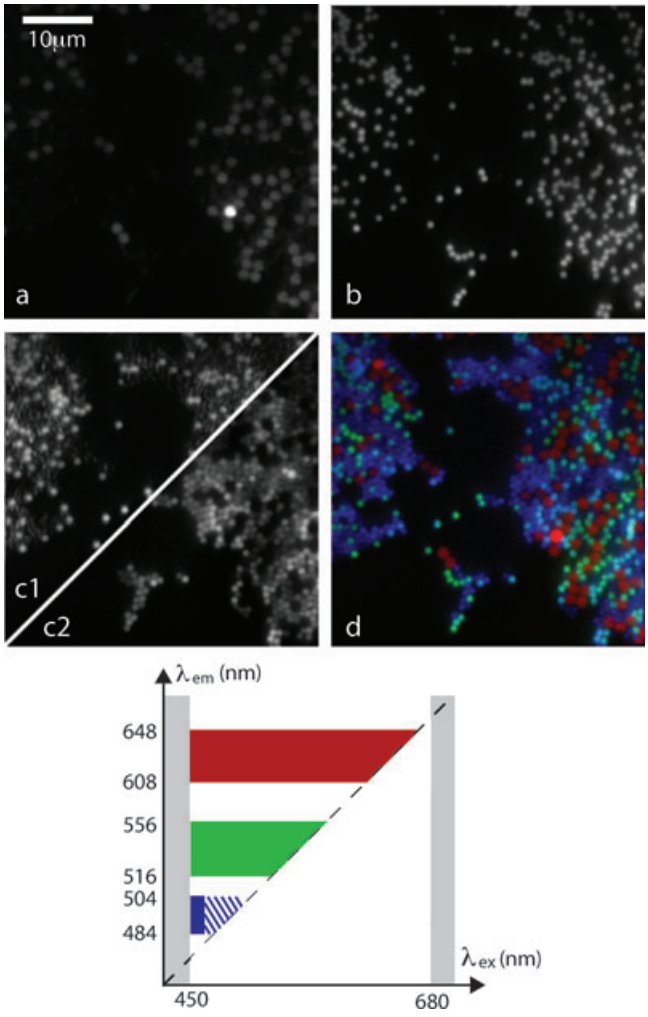


**Fig. 7.** Images of fluorescent beads mounted in immersion oil. (a) Red channel using 608-648nm emission filter. (b) Green channel using 516–556 nm emission filter. (c1) Blue channel using 484–504 nm emission filter, showing mainly emission from the green beads and scattered light from the other beads, whereas the weak blue fluorescence was obscured. (c2) Blue channel using 432–482 nm excitation and 484–504 nm emission filter. (d) Compound image constructed from images (a), (b) and (c2). The chart shows the spectral regions used in the corresponding image colour channels. The cross-hatched blue region was included in (c1) but excluded in (c2).

were employed. The amount of background scatter was similar for each specimen. For the images in Fig. 6, the specimen with the weakest fluorescence signal of those presented here, the background was approximately 37% as intense as the brightest pixels in the image.

Another detection combination is shown in Fig. 8, where excitation filtering is used in conjunction with spectrally resolved detection to measure fluorescence from quantum dots. The specimen consisted of a suspension of three species of CdSe/ZnS quantum dots (Evident EviDots) in toluene. Measurements were taken using the full spectrum and also

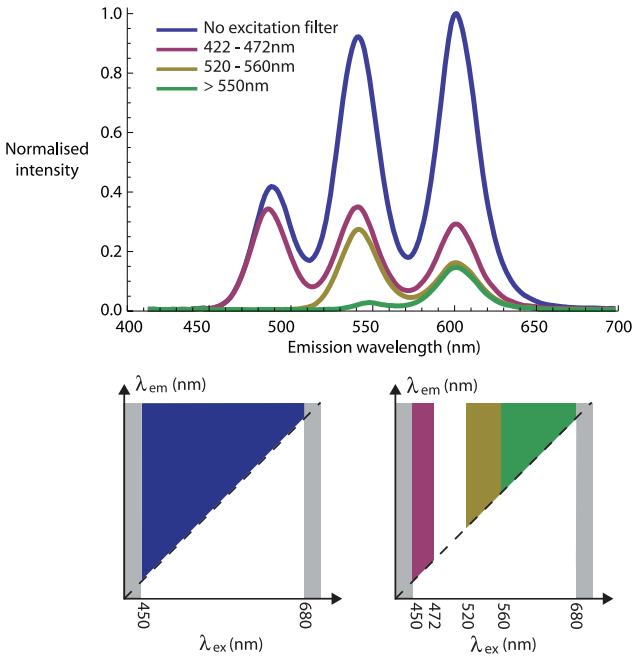


**Fig. 8.** Emission spectra of a specimen consisting of a suspension of three types of quantum dots in toluene. The nominal emission peaks of the dots were 482, 537 and 603 nm. The different excitation filters, detailed in the legend, were used to illustrate the dependence of the emission spectrum on the excitation range. The excitation/emission spectral charts show the regions of the spectrum used in the corresponding colour plot.

with three different excitation filters. The three distinct emission peaks of the quantum dots are apparent in the full spectrum measurement. The spectra obtained using filters show the dependence of the emission spectra on the excitation wavelength range. Note that all of the quantum dots have strong excitation response for the shorter wavelengths. As the excitation wavelength increases, only the longer wavelength emission remains.

## Discussion and conclusion

We have shown that through the combination of coherent illumination, pupil plane spatial filtering and polarization filtering, one can obtain full-spectrum fluorescence micrographs without the use of wavelength filters. Furthermore, in conjunction with SI, the microscope can produce three-dimensionally resolved, sectioned images with improved background rejection. As the separation of illumination and fluorescence is achromatic, the system can also be used with any combination of excitation filtering, emission filtering and spectral detection.

Although the pupil plane filtering method has some similarity to conventional dark field imaging, we emphasize that the present implementation is only practical using the high intensity, single spatial mode nature of the WLS source. Similar spectral coverage and total illumination power could

be produced using, for example, an arc lamp source in a K öhler illumination system. However, it would be impractical to generate the necessary single mode illumination with this source. Conversely, the WLS illumination is readily implemented using simple optics.

The use of polarization filtering leads to a significant increase of contrast between fluorescence and scattered light, albeit at the expense of some of the fluorescence intensity. Due to the depolarizing effect of the scattering process, it is also not possible to completely filter out scattered light in this way. Indeed, this microscope is most useful when imaging specimens that are either strongly fluorescent or weakly scattering. A complete assessment of the relative contribution of fluorescence and backscattered light to a full-spectrum image would require the differentiation of two types of light possessing the same wavelength. Introducing emission filters, we have shown that detected light corresponds closely to the expected distribution of fluorescence markers. The microscope was also used to acquire full emission spectra covering the same spectral range as the illumination. This configuration could be particularly useful when combined with multichannel spectral detection, as is available in several commercial microscope systems (see e.g. appendix 2 of Pawley 2006).

We conclude that this microscope could prove useful in applications where the full fluorescence spectrum must be acquired, without restriction to available wavelength filters or laser lines. It has greatest potential for the imaging of low scattering specimens with strong fluorescent signals. The simple practical implementation means that it is well suited for combination with existing microscope systems.

## Acknowledgements

This work was funded by the Biotechnology and Biological Sciences Research Council, UK (reference BB/E01240X/1). M.J.B. was supported by the Royal Academy of Engineering and the Engineering and Physical Sciences Research Council, UK (reference EP/E055818/1). A.J. was funded by the FWF Austrian Science Fund.

## References

Betz, T., Teipel, J., Koch, D., Hartig, W., Guck, J., Kas, J. & Giessen, H. (2005) Excitation beyond the monochromatic laser limit: simultaneous 3-D confocal and multiphoton microscopy with a tapered fiber as white-light laser source. *J. Biomed. Opt.* **10**, 54009.

Booth, M.J., Juskaitis, R. & Wilson, T. (2008) Spectral confocal reflection microscopy using a white light source. *J. Eur. Opt. Soc. Rap. Public.* **3**, 08026.

Born, M. & Wolf, E. (1983) *Principles of Optics*, 6th edn, Pergamon Press, Oxford.

Cai, L.Z., Liu, Q. & Yang, X.L. (2003) Phase-shift extraction and wave-front reconstruction in phase-shifting interferometry with arbitrary phase steps. *Opt. Lett.* **28**, 1808–1810.

Dunsby, C., Lanigan, P.M.P., McGinty, J., *et al.* (2004) An electronically tunable ultrafast laser source applied to fluorescence imaging and fluorescence lifetime imaging microscopy. *J. Phys. D-Appl. Phys.* **37**, 3296–3303.

Frank, J.H., Elder, A.D., Swartling, J., Venkitaraman, A.R., Jeyasekharan, A.D. & Kaminski, C.F. (2007) A white light confocal microscope for spectrally resolved multidimensional imaging. *J. Microsc.-Oxford* **227**, 203–215.

Gustafsson, M.G.L. (2000) Surpassing the lateral resolution limit by a factor of two using structured illumination microscopy. *J. Microsc.-Oxford* **198**, 82–87.

Karadaglic, D. & Wilson, T. (2008) Image formation in structured illumination wide-field fluorescence microscopy. *Micron* **39**, 808–818.

Lakowicz, J.R. (1999) *Principles of Fluorescence Spectroscopy*, 2nd edn, Kluwer/Plenum, New York.

McConnell, G., Poland, S. & Girkin, J.M. (2006) Fast wavelength multiplexing of a white-light supercontinuum using a digital micromirror device for improved three-dimensional fluorescence microscopy. *Rev. Scient. Instrum.* **77**, 013702.

Neil, M.A.A., Juskaitis, R. & Wilson, T. (1997) Method of obtaining optical sectioning by using structured light in a conventional microscope. *Opt. Lett.* **22**, 1905–1907.

Neil, M.A.A., Squire, A., Juskaitis, R., Bastiaens, P.I.H. & Wilson, T. (2000) Wide-field optically sectioning fluorescence microscopy with laser illumination. *J. Microsc.-Oxford* **197**, 1–4.

Owen, D.M., Auksorius, E., Manning, H.B., Talbot, C.B., de Beule, P.A.A., Dunsby, C., Neil, M.A.A. & French, P.M.W. (2007) Excitation-resolved hyperspectral fluorescence lifetime imaging using a UV-extended supercontinuum source. *Opt. Lett.* **32**, 3408–3410.

Pawley, J.B. (ed.) (2006) *Handbook of Biological Confocal Microscopy*, 3rd edn, Springer, New York.

Ye, J.Y., Divin, C.J., Baker, J.R. & Norris, T.B. (2007) Whole spectrum fluorescence detection with ultrafast white light excitation. *Opt. Express* **15**, 10 439–10 445.

Wolleschensky, R., Zimmermann, B. & Kempe, M. (2006) High-speed confocal fluorescence imaging with a novel line scanning microscope. *J. Biomed. Opt.* **11**, 064011.